

Fermilab E906/SeaQuest Drell-Yan Experiment

Kazutaka Nakahara for the Fermilab E906/SeaQuest Collaboration

University of Maryland College Park, Department of Physics, College Park, MD 20742-4111

Abstract. The E906/SeaQuest experiment will use the 120 GeV proton beam extracted from the Fermilab Main Injector to measure the Drell-Yan cross section in p-p, p-d, and p-A scattering. Data from liquid hydrogen and deuterium targets will be sensitive to the light anti-quark asymmetry, \bar{d}/\bar{u} , over a range of parton momentum fraction $0.04 < x < 0.45$. Previous measurements from the E866/NuSea experiment have shown that while there were clear signs of flavor asymmetry at moderate x , the quark sea became flavor symmetric at higher x , suggesting a possible shift in the underlying mechanism generating the sea. Measurements from solid nuclear targets (carbon, calcium, and tungsten) will determine the modification of antiquark distributions in the nucleus. The results, in addition to being complementary to similar measurements performed through deep inelastic scattering, will also be valuable in providing the nuclear corrections necessary to extract nucleon parton distribution functions from neutrino data. The experiment will start in 2011, and will run for two years.

Keywords: Drell-Yan, Parton Distributions, QCD, EMC Effect

PACS: 14.20.Dh, 14.65.Bt

INTRODUCTION

Extensive studies of parton distribution functions (PDFs) have been performed through both deep inelastic scattering (DIS) and Drell-Yan processes. Global fits¹ show the complementary nature of DIS and Drell-Yan in determining nucleon PDFs, as both data are sensitive to different combinations of distribution functions, providing essential roles in placing constraints on the PDFs. In particular, Drell-Yan experiments provide direct sensitivity to the sea quark distributions.

The Drell-Yan process, first observed at BNL/AGS in 1970², involves the production of a lepton anti-lepton pair from $q\bar{q}$ annihilation. The mass spectrum, from the E866/NuSea experiment³, can be seen in Fig. 1 with sufficient resolution to show hadronic resonances on top of a relatively smooth distribution of di-lepton (muon) pairs. The Drell-Yan cross section is

$$(1) \quad \frac{d^2\sigma}{dx_1 dx_2} = \frac{4\pi\alpha^2}{9x_1 x_2 s} \sum e_i^2 [\bar{q}(x_1)q(x_2) + q(x_1)\bar{q}(x_2)]$$

where x_1 and x_2 are the parton momentum fraction of the beam and the target, respectively, $q(x)$ and $\bar{q}(x)$ are the parton distributions, the sum is over quark flavor, and s is the square of the center of mass energy. This tree level expression accounts for approximately half of the measured cross-section, while QCD corrections from next-to-leading order (NLO) terms account for the other half. While the structure functions extracted from DIS contain both

quark and anti-quark contributions, the terms within the sum in Eq.1 can be kinematically separated such that the process is primarily sensitive to the target anti-quark, allowing for a direct means of probing the characteristics of the nucleon sea. Furthermore, the Drell-Yan process is an initial state interaction due to the timelike nature of the virtual photon. There are no final state QCD effects between the di-muons and the target or beam partons, allowing for a clean probe to study the structure of nucleons and nuclei.

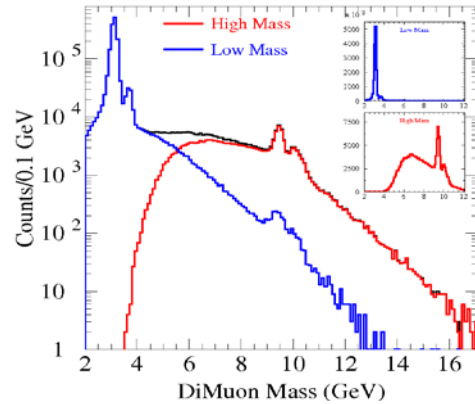


FIGURE 1. Di-muon mass spectrum for Drell-Yan scattering as seen by the E866/NuSea experiment³. The J/Ψ and upsilon resonances seen in the di-muon spectrum also received production contributions from gluon-gluon fusion. These mass regions, therefore, must be eliminated from the otherwise smooth distribution.

While E906/SeaQuest has numerous physics objectives, this manuscript will focus on the determination of \bar{d}/\bar{u} , the nuclear modification effect, and the significance of Drell-Yan measurements in the extraction of parton distribution functions from global fits.

PHYSICS MOTIVATION

Light Anti-quark Flavor Asymmetry

The \bar{d} and \bar{u} distributions within the nucleon give unique insight into the formation of the quark sea. While the non-perturbative nature of this sea poses a challenge in performing quantitative calculations, experiments have been performed to constrain the assumptions that underlie various phenomenological models.

A perturbative picture of the nucleon anti-quarks being generated through gluon splitting would suggest a symmetric sea; no known symmetry requires the equality of \bar{d} and \bar{u} distributions. However, a symmetric sea has been a common assumption until the New Muon Collaboration (NMC)⁴ measured the proton and neutron structure functions, F_2^p and F_2^n , and showed

$$\int_0^1 [F_2^p - F_2^n] dx = 0.235 \pm 0.026 \quad (2)$$

where a value of 1/3, referred to as the Gottfried Sum Rule (GSR)⁵, is expected in the case where $\bar{u} = \bar{d}$. While the E772 experiment⁶ was the first to use Drell-Yan scattering to set constraints on the \bar{d}/\bar{u} ratio, the NA51 experiment⁷ was the first to directly measure

$$\left. \frac{\bar{u}_p}{\bar{d}_p} \right|_{(x)=0.18} = 0.51 \pm 0.04 \pm 0.05 \quad (3)$$

to confirm the inequality of the two distributions. The Drell-Yan cross section ratio in proton-proton and proton-deuteron scattering, under assumptions of charge symmetry, $\bar{d}(x) \ll 4\bar{u}(x)$, and that the deuteron parton distribution can be expressed as a sum of proton and neutron distributions can be reduced to

$$\left. \frac{\sigma^{pd}}{\sigma^{pp}} \right|_{x_1 \gg x_2} \approx \frac{1}{2} \left(1 + \frac{\bar{d}(x_2)}{\bar{u}(x_2)} \right) \quad (4)$$

where, in a simple gluon splitting picture, this ratio would be equal to unity.

The E866/NuSea experiment extended the NA51 measurements by determining the light anti-quark ratio over a range of x . The experiment was performed at Fermilab using an 800 GeV proton beam extracted from the Tevatron. The results, seen in Fig. 2, show not just its agreement with the NA51 results, but also a drop in the ratio toward unity at higher x , suggesting that the underlying mechanism responsible for the sea maybe shifting. Calculations of $\int_0^1 \bar{d}(x) - \bar{u}(x) dx$ from the E866 results using values of $\bar{d} + \bar{u}$ obtained from the CTEQ¹ and MRS⁸ fits gives a result of 0.118 ± 0.012 consistent with and with higher precision than the NMC results.

There are several non-perturbative models that attempt to account for the inequality of the light anti-quark distributions. One such approach is the meson cloud model⁹ which models the proton as a nucleon with a cloud of mesons. A proton wave function with sizable $|N\pi\rangle$ states, for example, will then have an excess of \bar{d} quarks from the π^+ .

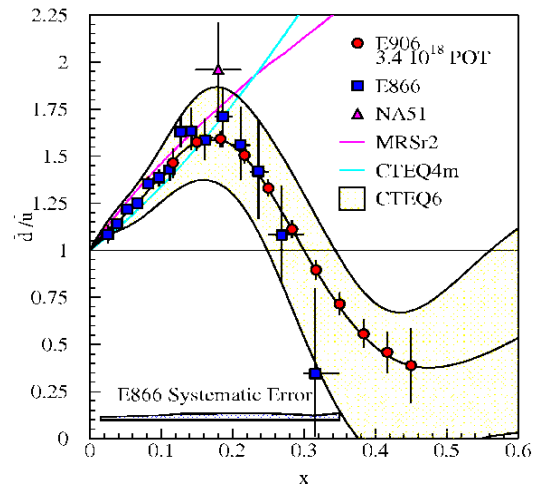


FIGURE 2. Results from the E866/NuSea¹⁰ and NA51 experiments, together with the expected kinematic range and uncertainties for the E906/SeaQuest experiment.

In chiral perturbation theory¹¹, a portion of the sea is generated when Goldstone bosons couple to the constituent quarks, such as $u \rightarrow d\pi^+$ and $d \rightarrow u\pi^-$. Here, the abundance of \bar{d} over \bar{u} is an artifact of the extra valence u quark of the proton.

These models, however, do not incorporate the effects of the flavor symmetric sea at higher x , leading to the over-prediction of the ratio. The drop-off of the ratio, therefore, could be resulting from a shift in the anti-quark production mechanism from non-perturbative processes toward perturbative processes, though this would imply a significantly

larger gluon distribution at high x than given by current global fits. While attempts to explain the kinematic behavior of the ratio have been made using phenomenological models, knowledge of the light anti-quark flavor asymmetry is primarily data-driven.

The E906/SeaQuest experiment will expand upon the E866/NuSea measurements with improved statistics and greater range in x , as shown in Fig. 2.

Nuclear Modification

The modification of nuclear cross sections of bound systems compared to those of free nucleons was first seen by the European Muon Collaboration (EMC)¹² through muon-induced DIS on an iron target. The effect has been observed across a wide variety of nuclear targets, and although various phenomenological models have been suggested as possible explanations, the underlying cause of the effect continues to be elusive. Fig. 3 shows the cross section ratio of calcium nuclei with respect to that of deuterium. The region above $x=0.3$ where a suppression of the cross section can be seen is typically called the "EMC Effect" region, while the strong suppression seen below $x=0.1$ is called the shadowing region. The intermediate region around $x=0.1-0.2$ where an enhancement of the cross section is seen is the anti-shadowing region.

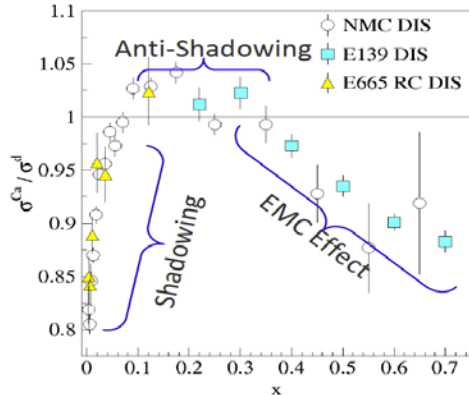


FIGURE 2. Nuclear modification effect for calcium nuclei with respect to that of deuterium, seen across three distinct kinematic regions by the NMC³, E139¹³, and E665¹⁴ experiments.

If the nuclear structure functions were to be modeled as a convolution of proton and neutron structure functions, it is possible to infer the origin of

the nuclear modification effect as being caused by either a modification of the individual nucleon structure functions when inside a nuclear medium, or due to multi-nucleon effects such as pion exchange and nuclear binding.

Models have been suggested that modifications in the nuclear structure functions between, say, iron and deuterium, maybe due to rescaling of the confinement radius^{15,16} of the nuclear constituents which originates from a relative shift in the scale of the measurements ($Q^2 \rightarrow \xi_A Q^2$). However, the model requires an increase in the nucleon radius greater than what was seen from inclusive electron-nucleus scattering¹⁷. Shadowing and anti-shadowing¹⁸ were initially predicted to be associated with the overlap of partons. Later studies have suggested that the recombination of gluons¹⁹ would screen the increasing parton density for heavier nuclei, resulting in a reduction in the cross section. The pion excess model²⁰, where the nucleons in a nuclear medium are bound together by the exchange of pions was suggested as a cause for the enhancement of the EMC ratio at small x . However, it is important to note that these models tend to only reproduce a portion of the kinematic range for which modification effects have been seen by experiment.

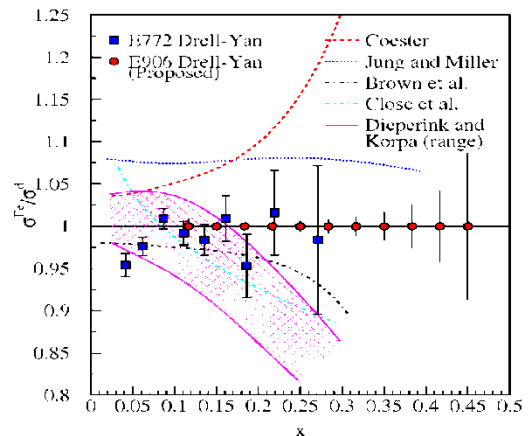


FIGURE 3. Nuclear modification results seen by E772, as well as expected uncertainties from E906. The various lines show predictions by Berger and Coester²¹ (pion model), Jung and Miller²² (pion model), Brown²³ (chiral model), Close²⁴ (rescaling model), and Deperink and Korpa²⁵ (pion model).

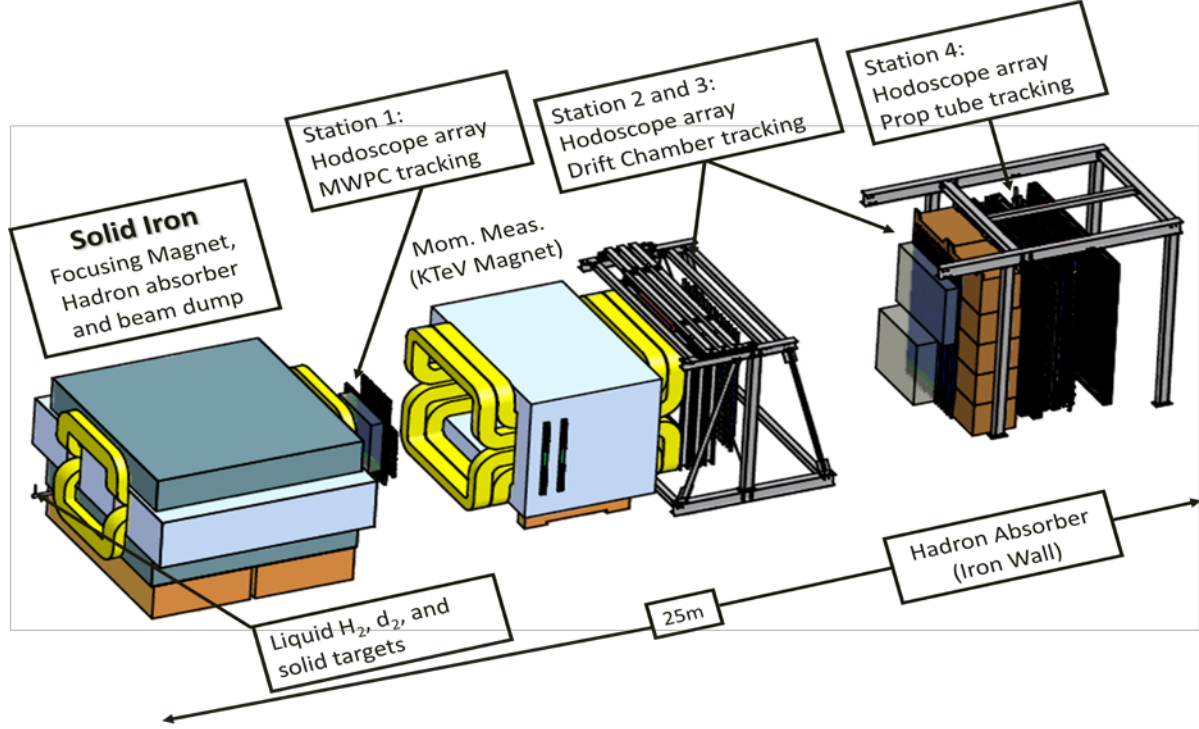


FIGURE 4. Schematic layout of the E906/SeaQuest Drell-Yan Spectrometer.

While structure functions extracted from DIS are sensitive to both quark and anti-quark contributions, efforts have been made via Drell-Yan measurements to isolate the sea contribution to the nuclear modification effect. The E772 experiment²⁶, performed at Fermilab using an 800 GeV proton beam, took Drell-Yan measurements over a range of momentum fraction $0.1 < x < 0.3$ and found that the anti-shadowing enhancement seen in DIS and expected from the pion model was not seen. The result suggests that the enhancement seen in the anti-shadowing region through DIS maybe a valence effect, or that the nuclear effects in the sea maybe different from those of the valence sector. The enhancement effects seen from DIS together with the lack of similar effects seen by Drell-Yan poses a challenge to phenomenological models that must be consistent with both results.

The E906/SeaQuest experiment will extend the E772 measurements to larger x , which will allow for comparisons between DIS and Drell-Yan results into the "EMC Effect" region.

Parton Distribution Functions

In addition to the Drell-Yan ratio measurements, the absolute proton-proton and proton-deuteron cross

sections will be determined. The cross sections can be expressed approximately as

$$\sigma^{pp} \propto 4u(x_1)\bar{u}(x_2) + d(x_1)\bar{d}(x_2) \quad (5)$$

$$\sigma^{pd} \propto [4u(x_1) + d(x_1)][\bar{u}(x_2) + \bar{d}(x_2)] \quad (6)$$

The cross section measurements will be sensitive to the beam proton over the range $0.3 < x_1 < 0.85$ and $0.1 < x_2 < 0.45$. The proton-deuteron cross section, therefore, is sensitive to the small x_2 absolute magnitude of the anti-quark sea, $\bar{d} + \bar{u}$, as well as the large x_1 structure function, $F_2^p \propto 4u(x) + d(x)$, obtained from electron/muon DIS measurements on a proton target. Furthermore, while these absolute cross sections provide a different combination of parton distributions compared to neutrino-nuclei DIS, the proton-nuclei measurements will provide insight into the nuclear corrections required for DIS measurements on deuterium as well as heavy targets.

E906/SEAQUEST

The E906/SeaQuest experiment will use the 120 GeV proton beam extracted from the Fermilab Main Injector. The spectrometer, seen in Fig. 4, borrows heavily from previous Drell-Yan experiments

performed at Fermilab. The experiment will receive 2×10^{12} protons/s for 5 seconds approximately each minute, with a total integrated charge of 3.4×10^{18} protons over 2 years distributed among seven targets.

As can be seen from Eq. 1, the Drell-Yan cross section scales as $1/s$, while the background rates scale as s . The use of a lower energy beam compared to E866/NuSea will, therefore, allow for a 50-fold increase in statistics over the predecessor experiment. This is particularly important in the high- x region, where results from previous experiments were limited by lack of statistics. While the lower beam energy is advantageous in improving the signal to noise, the lower energy also leads to increased probabilities for muonic decay of the produced hadrons. This is partially compensated by reducing the target-to-hadron absorber distance. Furthermore, lower energy muons will multiple scatter more easily in the hadron absorber. The systematic uncertainty for E906/SeaQuest is expected to be comparable to E866/NuSea, at approximately 1% in cross section ratio.

The beam will be incident on one of seven targets (liquid H_2 , liquid D_2 , empty cryogenic target, carbon, tungsten, calcium, and "no target"). The cryogenic target flasks are 20 inches long with a 3 inch diameter, which results in an approximately 10% interaction length with a luminosity of 3.4×10^{35} /cm²/s. The thickness of the solid nuclear targets is adjusted to match the interaction lengths of the liquid targets. The seven targets are mounted on a translation table which will change the target position between beam spills in order to remove systematic uncertainties from long term drifts in target or beam conditions.

The di-muons produced at the target are focused onto a set of four detector stations. The focusing magnet is also the beam dump and a hadron absorber in order to minimize the background seen by the detector stations. Each detector station consists of a set of hodoscope scintillator arrays to provide the di-muon trigger, and a set of wire chamber/proportional tubes. While many of the detectors are refurbished components that will be re-used from previous experiments, the top half of the station 3 chambers are newly fabricated. New station 3 chambers are designed to increase the overall acceptance of the spectrometer such that it is more sensitive to the high x region. In addition, while station 1 drift chambers from the E866/NuSea experiment are currently installed, new Multi-Wire-Proportional-Chambers (MWPCs) are being fabricated that can handle higher rates and provide increased kinematic acceptance. All hodoscope scintillators have been installed, and cosmic tests are on-going. Most of the wire chambers from previous

experiments have been refurbished and are ready for beam.

A momentum measuring magnet is placed between stations 1 and 2 in order to allow for the calculation of the di-muon momentum as their tracks are reconstructed in software. Final muon identification is provided by an absorber wall that is placed between the station 3 and 4 detectors, and is designed to reject all particles except muons.

The E906/SeaQuest data path roughly consists of five components. These include the trigger module which monitors the detectors for a prospective Drell-Yan event, a VME/CODA-based data acquisition (DAQ), a slow-control system, and a decoder and MySQL database.

The triggers from the hodoscope planes are sent to a trigger module where they are filtered to remove extraneous background events. All acceptable triggers are then sent to the VME data acquisition system. Further filtering of extraneous events will be performed later in software/analysis during track reconstruction.

The DAQ consists of 11 VME-based readout controllers (ROCs). One of the ROCs houses the trigger supervisor which distributes the trigger from the trigger module to the other 10 auxiliary ROCs. The auxiliary ROCs will contain a trigger interface card to communicate with the trigger supervisor, and custom-made time-to-digital convertors (TDCs) to receive the wire chamber/proportional tube signals. All TDCs will work on a common stop trigger, whereby the time difference between the wire chamber/proportional tube signal and the trigger is retrieved and written into the TDC memory buffer. The buffer is then read by the CEBAF Online Data Acquisition (CODA2.6.1)²⁷ and output to disk.

In addition to the DAQ which monitors the detectors, a slow-control system will monitor all other experimental conditions that may change at timescales longer than the trigger frequency. These include information regarding the target system and the beam, as well as detector high voltages and thresholds, which are logged twice a minute before and after the 5 second beam pulse, and inserted into the CODA datastream between the fast VME data. Finally, a decoder interprets and maps the encoded CODA file into wire chamber/proportional tube channels, and outputs the data into a MySQL database. To date, the full signal chain from the hodoscope scintillators to the MySQL database has been tested.

Simulations have been performed using both "Fast Monte Carlo" and GEANT-based Monte Carlo codes in order to ascertain the relevant event rates. In addition to the di-muon pairs, there will be approximately 100 random coincidences per spill of

two independent single muons originating primarily from π and K decaying in-flight. Most of these random di-muon triggers can be eliminated either in hardware by constraining the mass of the pair, or during analysis by applying cuts based on the reconstructed trajectory.

The analysis codes, which include both online monitoring and offline replay, are currently being refined through simulation while awaiting data.

SUMMARY

The E906/SeaQuest experiment will extend previous measurements of the light anti-quark flavor asymmetry and the nuclear modification effect with significantly improved statistics and kinematic range. The experiment will begin in 2011 and take data until the Fermilab upgrade shutdown which is slated to take place starting March 2012, after which the experiment will restart and run to completion.

ACKNOWLEDGMENTS

We would like to thank the Fermilab Particle Physics, and Accelerator Divisions for their assistance in performing this experiment. This work was supported in part by the U.S. Department of Energy Office of Nuclear Physics and the National Science Foundation.

REFERENCES

-
1. J. Pumplin et al., *JHEP* 07, 012 (2002)
 2. J. H. Christenson et al, *Phys. Rev. Lett.* 25, 21 (1970)
 3. E. A. Hawker et al., *Phys. Rev. Lett.* 80, 3715 (1998)
 4. P. Amaudruz et al., *Phys. Rev. Lett.* 66, 2712 (1991)
 5. K. Gottfried, *Phys. Rev. Lett.* 18, 1174 (1967)
 6. P. L. McGaughey et al., *Phys. Rev. Lett.* 69, 1726 (1992)
 7. A. Baldit et al., *Phys. Lett.* B332, 244 (1994)
 8. A. D. Martin, R. G. Roberts, W. J. Stirling, and R. S. Thorne, *Eur. Phys. J.* C39, 155 (2005)
 9. E. J. Eichten, I. Hinchliffe and C. Quigg, *Phys. Rev. D* 45, 2269 (1992)
 10. R. S. Towell, "Measurement of the Antiquark Flavor Asymmetry in the Nucleon Sea", Ph.D. Thesis, University of Texas at Austin, 2004.
 11. A. Szczurek, A. Buchmans and A. Faessler, *Jour. Phys. C; Nucl. Part. Phys.* 22, 1741 (1996)
 12. J. J. Aubert et al., *Phys. Lett.* B123, 275 (1983)
 13. R. G. Arnold, et al. *Phys. Rev. Lett.* 52, 727 (1984)
 14. M. R. Adams et al., *Z. Phys* C67, 403-410 (1995)
 15. O. Nachtmann, H. J. Pirner, *Z. Phys.* C 21, 277 (1984)
 16. F. E. Close, R. G. Roberts, G. G. Ross, *Phys. Lett.* B 129, 346 (1983)
 17. J. T. Londergan, A. W. Thomas, *Progress in Particle and Nuclear Physics* 41, 49 (1998)
 18. N. N. Nikolaev, V. L. Zakharov, *Phys. Lett.* B 55, 397 (1975)
 19. L. V. Gribov, E. M. Levin, M. G. Ryskin, *Nucl. Phys. B* 188, 555 (1981)
 20. C. H. Llewellyn Smith, *Phys. Lett.* B 128, 107 (1983)
 21. E. L. Berger and F. Coester, *Phys. Rev.* D32, 1071 (1985)
 22. H. Jung and G. A. Miller, *Phys. Rev.* C41, 659 (1990)
 23. F. E. Close et al., *Phys. Rev.* D31, 1004 (1985)
 24. G. E. Brown, et al., *Nucl. Phys.* A593, 295 (1995)
 25. A. E. L. Dieperink and Cl. L. Korpa, *Phys. Rev.* C55, 2665 (1997)
 26. D. M. Alde, H. W. Baer, T. A. Carey, G. T. Garvey, A. Klein, C. Lee, M. J. Leitch, J. W. Lillberg, P. L. McGaughey, C. S. Mishra, et al., *Phys. Rev. Lett.* 64, 2479 (1990)
 27. G. Heyes et al, *The CEBAF on-line data acquisition system*, CHEP Conference (1994)